

Probing new scalars with the lepton anomalous magnetic moment and the weak equivalence principle violation

Xitong Mei^{1,2}, Dongfeng Gao^{1,3,*}, Wei Zhao⁴, Jin Wang^{1,3,5,†} and Mingsheng Zhan^{1,3,5,‡}

1 State Key Laboratory of Magnetic Resonance and Atomic and Molecular Physics, Wuhan Institute of Physics and Mathematics, Innovation Academy for Precision Measurement Science and Technology, Chinese Academy of Sciences, Wuhan 430071, China

2 School of Physical Sciences, University of Chinese Academy of Sciences, Beijing 100049, China

3 Hefei National Laboratory, Hefei 230088, China

4 Shandong University of Aeronautics, Binzhou 256600, China

5 Wuhan Institute of Quantum Technology, Wuhan 430206, China

(Dated: January 24, 2025)

A new scalar particle with generic couplings to the standard-model particles is a possible source for the lepton anomalous magnetic moment and the violation of the weak equivalence principle. Here, one-loop contributions to the lepton anomalous magnetic moment, involving the scalar-photon and scalar-lepton couplings, are calculated. Then, with the recent experimental results of the electron anomalous magnetic moment, the muon anomalous magnetic moment, and the MICROSCOPE mission, we find that a scalar which couples merely to the photon or leptons can not be consistent with three experimental results. It has to couple to both the photon and leptons simultaneously. Improved constraints on scalar-lepton and scalar-photon couplings are set: $|\lambda_e| = (1.8 - 8.2) \times 10^{-6}$, $|\lambda_\mu| = (2.5 - 4.8) \times 10^{-4}$, and $|\lambda_\gamma| = (1.5 - 6.5) \times 10^{-14} \text{ eV}^{-1}$ or $(1.4 - 6.1) \times 10^{-13} \text{ eV}^{-1}$. We find that the naive scaling relationship between the scalar-muon coupling and the scalar-electron coupling is not favored by three experimental results. Furthermore, we show that the minimal standard-model extension by one scalar is also not favored for scalar mass below 10^4 eV .

I. INTRODUCTION

Many theories beyond the standard model (SM) of particle physics suggest the existence of additional spin-0 bosons, which could be motivated by various issues, e. g. axions in the strong CP problem [1–3], axion-like-particle candidates in dark matter detection [4], extensions in the scalar sector of the SM [5–8], moduli in string theory [9–11], and dilatons in gravitational physics [12, 13]. Such a broad class of particles can be involved in various kinds of couplings to the SM particles, which can be either fundamental or effective, depending on the specific mechanism associated with the sign of new physics. The search for such particles, and consequently constraining the mass and coupling parameters, can be carried out by various experimental methods [14, 15].

In particular, the lepton anomalous magnetic moment, with the rapid improvement of experimental measurements, has been used as a stringent probe for the hypothetical spin-0 bosons. The SM prediction of the lepton anomalous magnetic moment can be derived as a function of the fine structure constant α , and has been calculated in many studies (for example, see Refs. [16–18] for the electron, and Refs. [19–21] for the muon). The fine structure constant can be best measured by atomic recoil experiments. Applied to ^{133}Cs , the experiment gave the result $\alpha_{\text{Cs}}^{-1} = 137.035999046(27)$ [22]. Applied to ^{87}Rb , the experiment gave the result $\alpha_{\text{Rb}}^{-1} =$

$137.035999206(11)$ [23]. These two results differ by 5.5σ from each other. Accordingly, this would produce two different SM predictions of the electron anomalous magnetic moment: $a_e^{\text{SM}}(\alpha_{\text{Cs}}) = 1159652181.61(23) \times 10^{-12}$ and $a_e^{\text{SM}}(\alpha_{\text{Rb}}) = 1159652180.252(95) \times 10^{-12}$. The electron anomalous magnetic moment can also be directly measured with one-electron quantum cyclotrons, where the best result is $a_e^{\text{Meas}} = 1159652180.59(13) \times 10^{-12}$ [24]. Thus, for the electron, the discrepancies between the SM prediction and the measurement are

$$\delta a_e^{\text{EXP}}(\text{Cs}) = a_e^{\text{Meas}} - a_e^{\text{SM}}(\alpha_{\text{Cs}}) = -1.02(26) \times 10^{-12},$$

and

$$\delta a_e^{\text{EXP}}(\text{Rb}) = a_e^{\text{Meas}} - a_e^{\text{SM}}(\alpha_{\text{Rb}}) = 0.34(16) \times 10^{-12}. \quad (1)$$

The discrepancies are about 4.0σ for the ^{133}Cs recoil experiment and 2.1σ for the ^{87}Rb recoil experiment, respectively. In other words, there are signs of new physics at the 4.0σ level for the ^{133}Cs recoil experiment and at the 2.1σ level for the ^{87}Rb recoil experiment, although the signs are not so strong. For the muon, the discrepancy between the SM prediction and the measurement is found to be [25]:

$$\delta a_\mu^{\text{EXP}} = a_\mu^{\text{Meas}} - a_\mu^{\text{SM}} = 2.49(48) \times 10^{-9}, \quad (2)$$

which is about 5.2σ . In this case, the sign of new physics is quite strong. Suppose that the discrepancy between the SM prediction and the measurement for the lepton anomalous magnetic moments is caused by hypothetical spin-0 bosons. Then, the lepton anomalous magnetic moments could be used to constrain their masses and coupling parameters (for example, see Refs. [26–28]).

* Email: dfgao@wipm.ac.cn

† Email: wangjin@wipm.ac.cn

‡ Email: mszhan@wipm.ac.cn

On the other hand, high precision tests of the weak equivalence principle (WEP) violation can also be used to probe hypothetical spin-0 particles [12, 13, 29]. The MICROSCOPE mission [30, 31] has achieved the highest precision of the WEP test, where the Eötvös parameter η is measured to be

$$\eta(\text{Pt, Ti})^{\text{EXP}} = -1.5(2.7) \times 10^{-15}. \quad (3)$$

Although there is no sign of new physics even at the 1σ level, the result (3) can still be used to set useful constraints on new physics models. Suppose that the WEP violation is caused by new light scalar particles through their couplings to the SM particles. Then, the MICROSCOPE mission can set new constraints on such scalar particles [29, 32].

In this work, we investigate the possibility that a light scalar can account for the discrepancy (1) for the electron, the discrepancy (2) for the muon, and the WEP violation (3). Here, we concentrate on the scalar coupling to the photon and its Yukawa couplings to leptons. In that context, we restrict ourself to the scalar mass range below the electronic mass, where the light scalar is regarded as a dark matter candidate and gets more and more attentions from various experiments [14, 33, 34]. The advantage of combining these three experiments together lies in the fact that these three experiments cover all the four fundamental interactions in nature. We get new constraints on the new scalar particle, which could not be obtained by using either the lepton anomalous magnetic moment or the WEP violation individually. One of our important findings is that the new scalar has to couple to both the photon and leptons simultaneously. This indicates that the scalar-photon and scalar-lepton couplings are effective couplings and maybe come from some more fundamental coupling.

This paper is organized as follows. In Sec. II, we write down the Lagrangian with couplings to the SM particles. Then, the results of the one-loop contribution to lepton anomalous magnetic moments and the scalar contribution to the Eötvös parameter are summarized. Detailed calculations are given in Appendixes A and B. In Sec. III, we consider the cases where the new scalar couples either to the photon or to leptons alone. We find that scalar models with either scalar-photon coupling or scalar-lepton couplings can not be consistent with all three experimental results ((1), (2) and (3)) at the 2σ level. In Sec. IV, we discuss the case where the new scalar couples to both the photon and leptons simultaneously. Improved constraints on scalar-photon coupling and scalar-lepton couplings are found. The minimal SM extension model in the scalar sector, and the naive scaling relationship between scalar-muon coupling and scalar-electron coupling are not favored by three experimental results. Finally, conclusion and discussion are given in Sec. V.

II. THE SCALAR MODEL & CALCULATION FOR δa_l AND η

To be specific, let us work on the linear coupling model, where linear couplings between the new scalar ϕ and the SM particles are assumed. Following Ref. [13], the general interaction terms can be written as follows,

$$\mathcal{L}_{int} = \phi \left[\lambda_\gamma F_{\mu\nu} F^{\mu\nu} + \frac{\lambda_g \beta_3}{2g_3} F_{\mu\nu}^A F^{A\mu\nu} + \sum_{i=l,q} (\lambda_i + \gamma_{m_i} \lambda_g m_i) \bar{\psi}_i \psi_i \right], \quad (4)$$

where ψ_l stands for the lepton fields for $l = e, \mu$ and ψ_q stands for the quark fields for $q = u, d$. g_3 is the QCD gauge coupling, and β_3 is the β -function for g_3 . m_i denotes the fermionic masses (leptons and quarks). γ_{m_i} is the anomalous dimension due to the renormalization-group running of the quark masses. λ_γ and λ_g denote the couplings to the $U(1)$ photon and the $SU(3)$ gluons, respectively. λ_l denotes the dimensionless Yukawa coupling to leptons, and λ_q denotes the dimensionless Yukawa coupling to quarks. In total, there are six coupling parameters ($\lambda_\mu, \lambda_e, \lambda_\gamma, \lambda_u, \lambda_d$, and λ_g).

A. One-Loop Contribution to δa_l

Suppose that the discrepancy between the SM prediction and the measurement for the lepton anomalous magnetic moments, δa_l ($l = e$ or μ), is caused by the new scalar ϕ . Since the Yukawa coupling λ_l is assumed to be small, it is enough to consider the contribution from one-loop Feynman diagrams to δa_l .

At one-loop level, there exist two types of Feynman diagrams. One is called the Scalar-Lepton-Lepton loop diagram (Fig. 1) and the other is called the Scalar-Lepton-Photon loop diagram (Fig. 2). Using the Passarino-Veltman Renormalization [35, 36], we can calculate them. The details of the calculation are given in Appendix A. Here we summarize the main results.

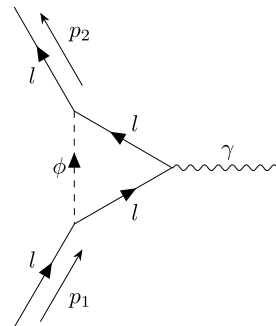


FIG. 1. The Scalar-Lepton-Lepton loop diagram

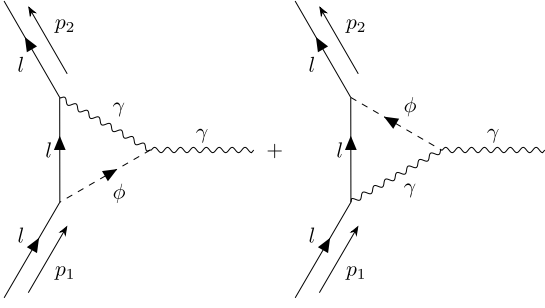


FIG. 2. The Scalar-Lepton-Photon loop diagrams

For the Scalar-Lepton-Lepton loop diagram, its contribution to δa_i is calculated to be

$$\delta a_{i1}(m_\phi) = \lambda_l^2 a_{sl}(r_l), \quad (5)$$

with

$$a_{sl}(r_l) = \begin{cases} \frac{-2r_l^2 - 3r_l^2 \log(r_l^2) + r_l^4 \log(r_l^2) - 2\sqrt{4r_l^2 - r_l^4} r_l^2 \cos^{-1}(\frac{r_l}{2}) + 2\sqrt{4r_l^2 - r_l^4} \cos^{-1}(\frac{r_l}{2}) + 3}{16\pi^2} & \text{if } r_l \leq 2, \\ \frac{-2r_l^2 - 3r_l^2 \log(r_l^2) + r_l^4 \log(r_l^2) - 2\sqrt{r_l^4 - 4r_l^2} r_l^2 \cosh^{-1}(\frac{r_l}{2}) + 2\sqrt{r_l^4 - 4r_l^2} \cosh^{-1}(\frac{r_l}{2}) + 3}{16\pi^2} & \text{if } r_l \geq 2. \end{cases} \quad (6)$$

Here $r_l \equiv m_\phi/m_l$, where m_ϕ is the mass for ϕ . In Ref. [27], the authors calculated the same diagram. Our result is consistent with theirs.

Similarly, the contribution from the Scalar-Lepton-

Photon loop diagrams is found to be

$$\delta a_{i2}(m_\phi) = \lambda_l \lambda_\gamma m_l b_{sl\gamma}(r_l), \quad (7)$$

with

$$b_{sl\gamma}(r_l) = \begin{cases} \frac{-2r_l^2 - 6r_l^2 \log(r_l^2) + r_l^4 \log(r_l^2) - 2\sqrt{4r_l^2 - r_l^4} r_l^2 \cos^{-1}(\frac{r_l}{2}) + 8\sqrt{4r_l^2 - r_l^4} \cos^{-1}(\frac{r_l}{2}) + 18}{48\pi^2} & \text{if } r_l \leq 2, \\ \frac{-2r_l^2 - 6r_l^2 \log(r_l^2) + r_l^4 \log(r_l^2) - 2\sqrt{r_l^4 - 4r_l^2} r_l^2 \cosh^{-1}(\frac{r_l}{2}) + 8\sqrt{r_l^4 - 4r_l^2} \cosh^{-1}(\frac{r_l}{2}) + 18}{48\pi^2} & \text{if } r_l \geq 2. \end{cases} \quad (8)$$

Then, the total one-loop contribution of the scalar field to δa_i is

$$\delta a_i = \delta a_{i1} + \delta a_{i2} = \lambda_l^2 a_{sl}(r_l) + \lambda_l \lambda_\gamma m_l b_{sl\gamma}(r_l). \quad (9)$$

One can see that λ_l appears in both terms, and λ_γ appears only in the second term. Note that, at one-loop level, δa_i does not get contributions from the scalar-quark coupling λ_q and the scalar-gluon coupling λ_g .

It is also worth noticing the behaviors of $a_{sl}(r_l)$ and $b_{sl\gamma}(r_l)$ as functions of r_l . As shown in Fig. 3, both $a_{sl}(r_l)$ and $b_{sl\gamma}(r_l)$ are positive for $m_\phi < m_e$, which is the mass range we focus on in this work.

B. Contribution of the scalar ϕ to η

The ϕ contribution to the Eötvös parameter has been calculated in Refs. [13, 37]. The summary of the calculation is given in Appendix B. Here, we quote the results as follows.

For two test bodies freely falling towards the Earth, the Eötvös parameter η is found to be

$$\eta = \left(1 + \frac{R_E}{\Lambda_\phi}\right) I\left(\frac{R_E}{\Lambda_\phi}\right) (\zeta_A - \zeta_B) \zeta_E e^{-R_E/\Lambda_\phi},$$

$$I(x) \equiv \frac{3(x \cosh(x) - \sinh(x))}{x^3}, \quad (10)$$

where R_E is the radius of the Earth, $\Lambda_\phi \equiv \hbar/m_\phi$ is the Compton wavelength of the scalar ϕ . $\zeta_{A,B}$ is the so-called scalar-charge for a mass, which is given in Eq. (B3). ζ_E is the scalar-charge for the Earth, which is

$$\zeta_E = -1.808 \times 10^{18} \lambda_e + 2.319 \times 10^{25} \lambda_\gamma \cdot \text{eV} - 3.133 \times 10^{27} \lambda_g \cdot \text{eV} - 3.973 \times 10^{19} \lambda_d - 3.967 \times 10^{19} \lambda_u \quad (11)$$

According to Refs. [29–31], the MICROSCOPE mission result (3) was achieved for a pair of test masses, which have different compositions [PtRh(90/10) and TiAlV(90/6/4) alloys]. The scalar-charges for them are

$$\zeta_{\text{Pt}} = -1.496 \times 10^{18} \lambda_e + 5.766 \times 10^{25} \lambda_\gamma \cdot \text{eV} \quad (12)$$

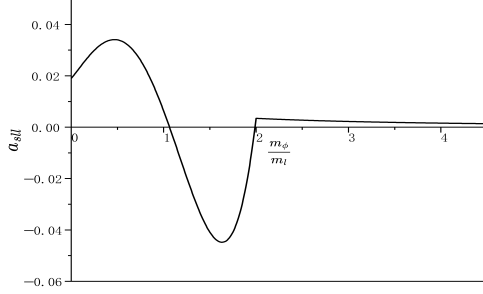
$$-3.149 \times 10^{27} \lambda_g \cdot \text{eV} - 4.320 \times 10^{19} \lambda_d - 4.231 \times 10^{19} \lambda_u$$

$$\zeta_{\text{Ti}} = -1.707 \times 10^{18} \lambda_e + 3.101 \times 10^{25} \lambda_\gamma \cdot \text{eV} \quad (13)$$

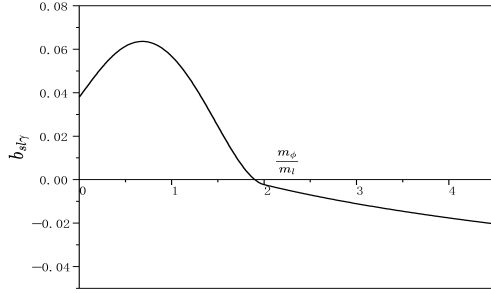
$$-3.159 \times 10^{27} \lambda_g \cdot \text{eV} - 4.159 \times 10^{19} \lambda_d - 4.123 \times 10^{19} \lambda_u$$

With Eqs. (10–13), one can write down the Eötvös parameter $\eta(\text{Pt}, \text{Ti})$ for the MICROSCOPE mission

$$\eta(\text{Pt}, \text{Ti}) = \left(1 + \frac{R_E}{\Lambda_\phi}\right) I\left(\frac{R_E}{\Lambda_\phi}\right) e^{-R_E/\Lambda_\phi} \quad (14)$$



(a)



(b)

FIG. 3. (a) The behavior of $a_{sl}(r_l)$. (b) The behavior of $b_{sl\gamma}(r_l)$.

$$\begin{aligned} & \times (-1.808 \times 10^{18} \lambda_e + 2.319 \times 10^{25} \lambda_\gamma \cdot \text{eV} \\ & - 3.133 \times 10^{27} \lambda_g \cdot \text{eV} - 3.973 \times 10^{19} \lambda_d - 3.967 \times 10^{19} \lambda_u) \\ & \times (2.115 \times 10^{17} \lambda_e + 2.664 \times 10^{25} \lambda_\gamma \cdot \text{eV} \\ & + 9.823 \times 10^{24} \lambda_g \cdot \text{eV} - 1.613 \times 10^{18} \lambda_d - 1.087 \times 10^{18} \lambda_u) \end{aligned}$$

It is clear that Eq. (14) depends on five coupling parameters ($\lambda_e, \lambda_\gamma, \lambda_u, \lambda_d$, and λ_g), which is very different to the case of Eq. (9), where δa_l depends only on three coupling parameters (λ_e, λ_μ and λ_γ).

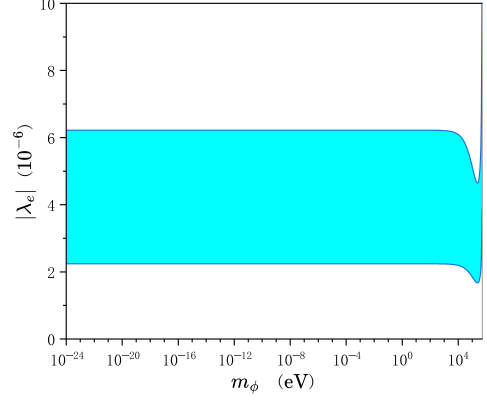
To fully utilize these three experimental results ((1), (2) and (3)), let us mainly focus on the scalar-photon coupling λ_γ and the scalar-lepton couplings (λ_e and λ_μ) in the following. In other words, we restrict our attention to the subspace, determined by $\lambda_u = \lambda_d = \lambda_g = 0$, of the full six-dimensional parameter space. In this subspace, Eq. (14) is reduced to

$$\begin{aligned} \eta'(\text{Pt, Ti}) = & \left(1 + \frac{R_E}{\Lambda_\phi}\right) I\left(\frac{R_E}{\Lambda_\phi}\right) e^{-\frac{R_E}{\Lambda_\phi}} (-3.824 \times 10^{35} \lambda_e^2 \\ & + 6.179 \times 10^{50} \lambda_\gamma^2 \cdot \text{eV}^2 - 4.328 \times 10^{43} \lambda_e \lambda_\gamma \cdot \text{eV}) \end{aligned} \quad (15)$$

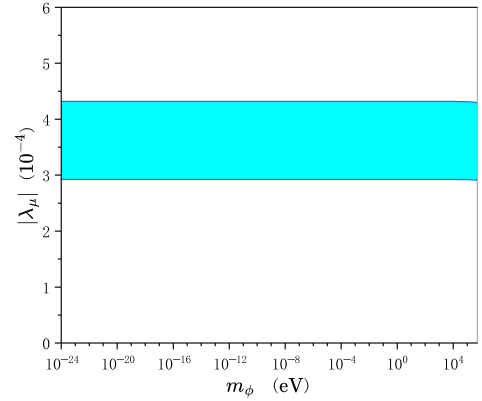
Note that, in the following, constraints on coupling parameters are set at the 2σ level, which is the common confidential level of new physics for all three experimental results.

III. INCOMPATIBILITY WITH THREE EXPERIMENTAL RESULTS FOR CASES WITH EITHER λ_γ OR λ_l ONLY

First, let us consider the case with λ_γ coupling parameter only. According to Eq. (9), it is easy to see that $\delta a_l = 0$. Obviously, this case is incompatible with results (1) and (2). But, according to Eq. (15), it is OK with the result (3). In one word, it can not be consistent with all three experimental results.



(a)



(b)

FIG. 4. (a) Constraint on λ_e set by the experimental result (1). (b) Constraint on λ_μ set by the experimental result (2). The allowed regions are shown in blue.

Next, let us consider the case with λ_l coupling parameter only. With Eq. (9), it is straightforward to find out constraints on λ_e set by the experimental result (1) and on λ_μ set by the experimental result (2), as shown in Figs. 4(a) and 4(b). It looks OK with experimental results (1) and (2).

Then, inserting the constraint on λ_e (shown in Fig. 4(a)) into Eq. (15), we would get a constraint on η , as shown in Fig. (5). Compared with the MICROSCOPE

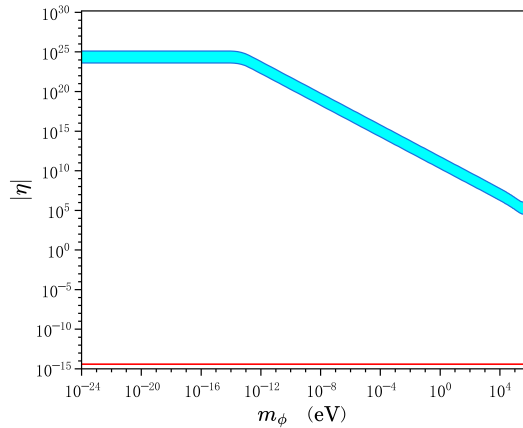


FIG. 5. Constraint on η set by the experimental result (1), where the allowed region is shown in blue. As comparison, the MICROSCOPE result (3) is shown in red.

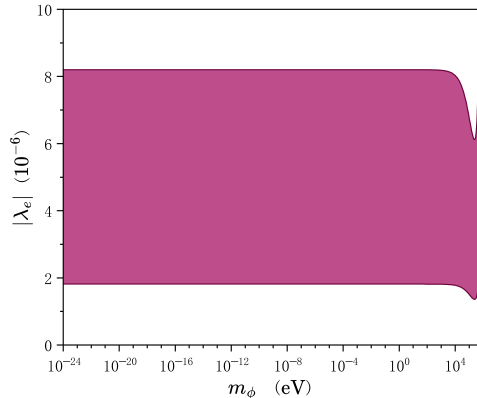
result (3), there exists a huge inconsistency. This shows that the model with only λ_l coupling could be consistent with two lepton anomalous magnetic moment measurements, but can not satisfy all three experimental results simultaneously.

The above two cases force us to consider the case with both λ_γ and λ_l couplings, which is the subject of the following section.

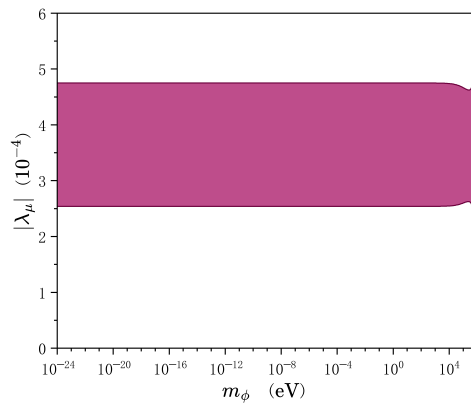
IV. FULL CONSTRAINTS ON λ_e , λ_μ AND λ_γ WITH ALL THREE EXPERIMENTAL RESULTS

A. Constraints on individual parameters

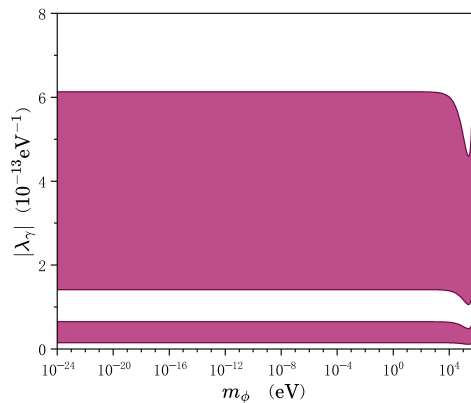
With three independent experimental results, we can fully constrain all three coupling parameters: λ_e , λ_μ and λ_γ . Inserting results (1), (2) and (3) into Eqs. (9) and (15), we can solve them and find out the constraints, as shown in Figs. 6(a), 6(b) and 6(c). One can see that, for the scalar mass below 10^4 eV, the allowed regions for all three coupling parameters are flat straps. In other words, constraints on three coupling parameters are almost independent of the scalar mass for $m_\phi < 10^4$ eV. For $|\lambda_e|$, the constraint is $(1.8 - 8.2) \times 10^{-6}$. For $|\lambda_\mu|$, the constraint is $(2.5 - 4.8) \times 10^{-4}$. For $|\lambda_\gamma|$, the constraints are $(1.5 - 6.5) \times 10^{-14}$ eV $^{-1}$ and $(1.4 - 6.1) \times 10^{-13}$ eV $^{-1}$. Clearly, all three coupling parameters are nonzero at the 2σ level, which shows sign of new physics. The reason is mainly attributed to the muon anomalous magnetic moment measurement (2), which indicates a 5.2σ confidential level of new physics. The results here again confirm our discussion in Sec. III, which states that the model with either λ_γ or λ_l alone can not be consistent with all three experimental results.



(a)



(b)

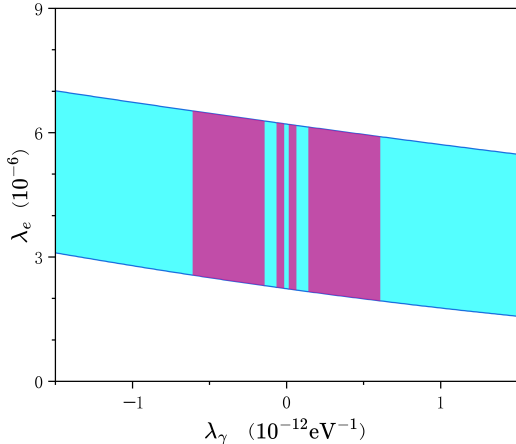


(c)

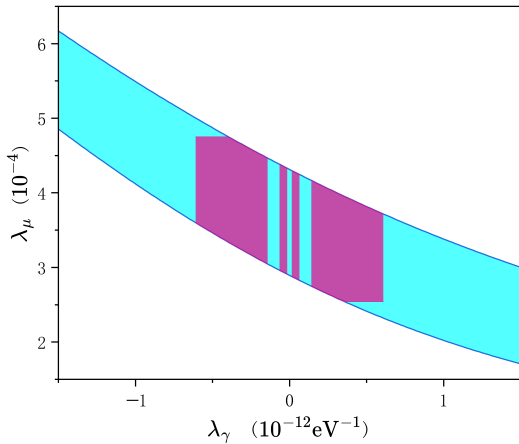
FIG. 6. (a) Full constraint on λ_e . (b) Full constraint on λ_μ . (c) Full constraint on λ_γ . The allowed regions are shown in violet.

B. Constraints on parameter pairs

After constraints on individual parameters are found, we continue to investigate correlations among three coupling parameters.



(a)



(b)

FIG. 7. (a) Constraint on the λ_e - λ_γ pair. (b) Constraint on the λ_μ - λ_γ pair. The allowed regions determined by all three experimental results are shown in violet. As comparison, the allowed regions determined by lepton anomalous magnetic moment measurement alone are shown in blue. Without losing generality, we have taken a typical value $m_\phi = 10^{-14}$ eV to draw the figures.

Constraints on the λ_e - λ_γ and λ_μ - λ_γ pairs are shown in Fig. 7. Actually, according to Eq. (9), the lepton anomalous magnetic moment measurements alone can be used to set constraints on the λ_e - λ_γ and λ_μ - λ_γ pairs, which are shown as blue regions in Fig. 7. Compared with blue regions which spread a large area in parameter space, the violet regions only cover finite areas. This greatly con-

fine the allowed parameter region, which clearly shows the advantage of putting all three experimental results together to constrain the scalar model.

Another interesting issue is about the so-called naive scaling [38]. It states that contributions from new physics to lepton anomalous magnetic moments scale with the square of lepton masses. In other words, naive scaling indicates that $\delta a_\mu/\delta a_e = (m_\mu/m_e)^2$. In Eq. (9), one has $a_{see} = a_{s\mu\mu}$ and $b_{se\gamma} = b_{s\mu\gamma}$ for $m_\phi < m_e$. Then, naive scaling implies that $\lambda_\mu/\lambda_e = m_\mu/m_e$. In Fig. 8, $|\lambda_\mu/\lambda_e|$ versus m_ϕ diagram is drawn. Clearly, it shows that naive scaling is not favored by three experimental results.

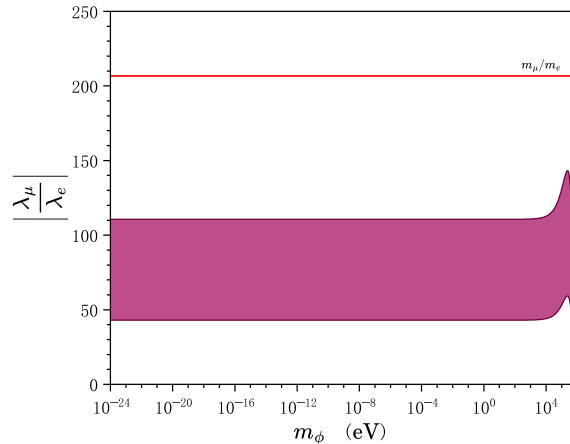


FIG. 8. Constraint on the ratio λ_μ/λ_e , where the violet region is the allowed region. The red line is the naive scaling value, m_μ/m_e .

C. The minimal SM extension by one scalar

In this subsection, let us focus particularly on a class of scalar models, which introduce new scalars by extending the scalar sector of the SM. In the minimal extension of the SM scalar sector [5–8], it contains an additional real scalar field with no gauge quantum numbers. Such a scalar field does not couple to the SM particles directly but rather through its mixing with the Higgs field. The relevant part of the Lagrangian is the following [8]

$$V_\varphi = -\frac{m_h^2}{2}H^\dagger H + \lambda_h(H^\dagger H)^2 + A\varphi H^\dagger H + \frac{m_\varphi^2}{2}\varphi^2,$$

where H stands for the Higgs field, and A stands for the coupling parameter between H and the new scalar field φ .

After spontaneous symmetry breaking, one has two vacuum expectation values, $\langle H^\dagger H \rangle = v^2/2$ and $\langle \varphi \rangle = \varphi_0$, with $v = 246$ GeV. Following the notations in Ref. [8], the above interaction will induce some effective cou-

plings between the scalar and the SM fields, which is

$$\mathcal{L}_{eff} = \frac{Av}{m_h^2} \left(g_{hff} \bar{f}f + \frac{g_{h\gamma\gamma}}{v} F_{\mu\nu} F^{\mu\nu} + \dots \right) \phi, \quad (16)$$

where $\phi \equiv \varphi - \varphi_0$. g_{hff} stands for the Yukawa couplings of the Higgs field to the SM fermions, and $g_{h\gamma\gamma}$ stands for the effective coupling of the Higgs field to the electromagnetic field. In the SM, $g_{hq} = m_q/v$ for quarks, $g_{hl} = m_l/v$ for leptons, and $g_{h\gamma\gamma} \simeq \alpha/(8\pi)$.

Compared to our notations, it is easy to write down the translation between them

$$\lambda_\gamma = \frac{A}{m_h^2} g_{h\gamma\gamma}, \quad \lambda_i = \frac{Av}{m_h^2} g_{hff}. \quad (17)$$

Of course, λ_γ , λ_e and λ_μ are not independent to each other. They should satisfy the following relations

$$\begin{aligned} \lambda_e/\lambda_\gamma &= v g_{hee}/g_{h\gamma\gamma} = 8\pi m_e/\alpha = 1.8 \times 10^9 \text{ eV}, \\ \lambda_\mu/\lambda_\gamma &= v g_{h\mu\mu}/g_{h\gamma\gamma} = 8\pi m_\mu/\alpha = 3.6 \times 10^{11} \text{ eV} \end{aligned} \quad (18)$$

One can easily see that the naive scaling, $\lambda_\mu/\lambda_e = m_\mu/m_e$, is satisfied for the model (16).

Actually, since there is only one coupling parameter A in the model, the experimental results (1) and (2) can set two independent bounds for A , by inserting Eq. (17) into Eq. (9). As shown in Fig. 9, the allowed region set by the result (1) is drawn in blue, and the allowed region set by the result (2) is drawn in green. Clearly, there is a very narrow overlap between the two allowed ranges. For $m_\phi < 10^4$ eV, there is no overlap at all. This means that the minimal SM extension by one scalar is not in favor for $m_\phi < 10^4$ eV. Note that this statement holds for the whole six-dimensional parameter space spanned by $\lambda_\mu, \lambda_e, \lambda_\gamma, \lambda_u, \lambda_d$, and λ_g , since δa_l does not depend on the scalar-quark coupling λ_q and the scalar-gluon coupling λ_g .

V. CONCLUSION AND DISCUSSION

The lepton anomalous magnetic moment together with the WEP violation involve all the four fundamental interactions in nature. Suppose that discrepancies between the SM predictions and measurements for the lepton (electron and muon) anomalous magnetic moments, and the WEP violation are all caused by a new scalar. By combining these three experiments together, we get new constraints on the new scalar, which could not be obtained by using either the lepton anomalous magnetic moment or the WEP violation alone. First, we find that the new scalar has to couple to both the photon and leptons simultaneously. Second, we show that the naive scaling relationship between the scalar-muon coupling and the scalar-electron coupling is not favored by three experimental results. Furthermore, the minimal SM extension by one scalar is also not favored for $m_\phi < 10^4$ eV.

For the electron anomalous magnetic moment, new measurement is ongoing to realize new precision [24].

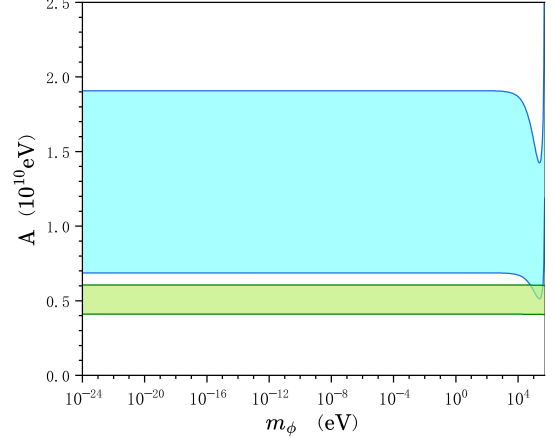


FIG. 9. Constraint on A , where the blue region is the allowed region set by the result (1), and the green region is the allowed region set by the result (2).

Analysis of the remaining data for the muon anomalous magnetic moment is underway and is expected to give further improvement in statistical precision [25]. Moreover, some space-based proposals, such as STE-QUEST [39], plan to push the WEP test to the 10^{-17} -level with atom interferometry. Thus, one could expect to set better bounds on the new scalar in the future.

ACKNOWLEDGMENTS

This work was supported by the Technological Innovation 2030 "Quantum Communication and Quantum Computer" Major Project (Grants No. 2021ZD0300603 and No. 2021ZD0300604), the Hubei Provincial Science and Technology Major Project (Grant No. ZDZX2022000001), and the Shandong Provincial Natural Science Foundation (Grant No. ZR2023QA143).

Appendix A: Calculation of one loop contribution to δa_l

We work on the linear coupling model, where linear couplings between the new scalar ϕ and the SM particles are assumed. Following Ref. [13], the general interaction terms can be written as follows,

$$\begin{aligned} \mathcal{L}_{int} = & \phi \left[\lambda_\gamma F_{\mu\nu} F^{\mu\nu} + \frac{\lambda_g \beta_3}{2g_3} F^A{}_{\mu\nu} F^{A\mu\nu} \right. \\ & \left. + \sum_{i=l,q} (\lambda_i + \gamma_{m_i} \lambda_g m_i) \bar{\psi}_i \psi_i \right]. \end{aligned} \quad (A1)$$

Note that the relation between notations used in Ref. [13] and ours is: $\lambda_\gamma \equiv \kappa d_e$, $\lambda_g \equiv -\kappa d_g$, $\lambda_i \equiv -\kappa m_i d_{m_i}$, where $\kappa \equiv \sqrt{4\pi G}$. The corresponding Feynman rules are given in Fig. 10.

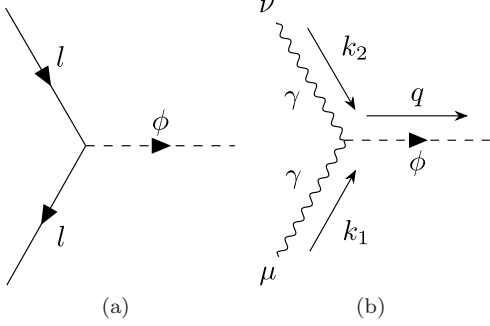


FIG. 10. (a) The Scalar-Lepton-Lepton Vertex: $i\lambda_e$. (b) The Scalar-Photon-Photon Vertex: $4i\lambda_\gamma[k_1^\nu k_2^\mu - g^{\mu\nu} k_1 \cdot k_2]$.

As discussed in [40], one can obtain various form factors F_i 's extracted from the lepton-photon vertex $\Gamma^\mu = \gamma^\mu F_1(q^2) + \frac{i\sigma^{\mu\nu}}{2m_l} q_\nu F_2(q^2) + \frac{i\sigma^{\mu\nu}}{2m_l} q_\nu \gamma_5 F_3(q^2) + \frac{1}{2m_l} (q^\mu - \frac{q^2}{2m_l} \gamma^\mu) \gamma_5 F_4(q^2)$, where q is the momentum of the external photon with on-shell condition $q^2 = 0$. The lepton anomalous magnetic moment a_l is defined to be

$$\begin{aligned} a_l &\equiv \text{Re}(F_2(0)), \\ \delta a_l &\equiv a_l - a_l^{\text{SM}}, \end{aligned} \quad (\text{A2})$$

where the SM prediction a_l^{SM} has been calculated in many studies (for example, see Refs. [16–18] for the electron, and Refs. [19–21] for the muon).

At one-loop level, two types of Feynman diagrams contribute to δa_l : the Scalar-Lepton-Lepton loop diagram (Fig. 11), and the Scalar-Lepton-Photon loop diagram (Fig. 12). We denote contributions of the former diagram as δa_{l1} , and the latter as δa_{l2} . Then, we have

$$\delta a_l = \delta a_{l1} + \delta a_{l2} \equiv \text{Re}(F_2^{(1)}(0) + F_2^{(2)}(0)), \quad (\text{A3})$$

where $F_2^{(i)}$ stands for the form factors of the two diagrams.

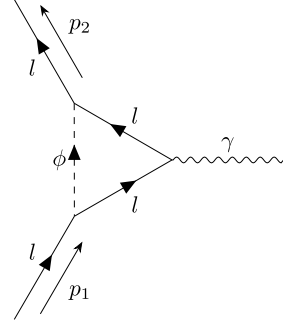


FIG. 11. The Scalar-Lepton-Lepton loop diagram

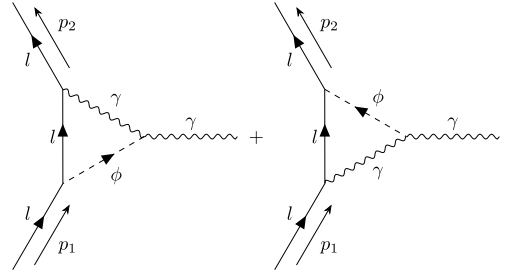


FIG. 12. The Scalar-Lepton-Photon loop diagrams

Let us first calculate the Scalar-Lepton-Lepton loop diagram (Fig. 11), using the Passarino-Veltman Renormalization [35, 36]. With the help of FeynCalc [41, 42] and FeynArts [43], we can derive the amplitude of Fig. 11 :

$$\begin{aligned} \text{Amp01} &= 2i\pi^2 e\lambda_l^2 m_l (p_1^\mu + p_2^\mu) [2C_1(m_l^2, 0, m_l^2, m_\phi^2, m_l^2, m_l^2) + C_{11}(m_l^2, 0, m_l^2, m_\phi^2, m_l^2, m_l^2) \\ &+ C_{12}(m_l^2, 0, m_l^2, m_\phi^2, m_l^2, m_l^2)] (\varphi(p_2, m_l)) \cdot (\varphi(p_1, m_l)) - i\pi^2 e\lambda_l^2 [B_0(0, m_l^2, m_l^2) + m_\phi^2 C_0(0, m_l^2, m_l^2, m_l^2, m_\phi^2) \\ &- 4m_l^2 C_0(0, m_l^2, m_l^2, m_l^2, m_l^2, m_\phi^2) - 2C_{00}(m_l^2, 0, m_l^2, m_\phi^2, m_l^2, m_l^2)] (\varphi(p_2, m_l)) \cdot \gamma^\mu \cdot (\varphi(p_1, m_l)), \end{aligned} \quad (\text{A4})$$

where $\varphi(p_i, m_e)$ stands for the electron field, p_1 is the incoming momentum of the lepton and p_2 is the outgoing

momentum. The involved one-point, two-point and three-point Passarino-Veltman coefficient functions are defined as follows

$$A_0(m_0^2) = \mu^{2\epsilon} \int \frac{d^d k}{(2\pi)^d} \frac{1}{k^2 - m_0^2 + i\epsilon}, \quad (\text{A5})$$

$$B_{\{0,\mu,\mu\nu\}}(p^2; m_0^2, m_i^2) = \mu^{2\epsilon} \int \frac{d^d k}{(2\pi)^d} \frac{\{1, k_\mu, k_\mu k_\nu\}}{(k^2 - m_0^2 + i\epsilon)((k+p)^2 - m_i^2 + i\epsilon)}, \quad (\text{A6})$$

$$C_{\{0,\mu,\mu\nu\}}(p_1^2, q^2, p_2^2; m_0^2, m_1^2, m_2^2) = \mu^{2\epsilon} \int \frac{d^d k}{(2\pi)^d} \frac{\{1, k_\mu, k_\mu k_\nu\}}{(k^2 - m_0^2 + i\epsilon)((k+p_1)^2 - m_1^2 + i\epsilon)((k+p_2)^2 - m_2^2 + i\epsilon)}, \quad (\text{A7})$$

$$C_\mu = p_{1\mu} C_1 + p_{2\mu} C_2, \quad (\text{A8})$$

$$C_{\mu\nu} = g_{\mu\nu} C_{00} + p_{1\mu} p_{1\nu} C_{11} + p_{2\mu} p_{2\nu} C_{22} + (p_{1\mu} p_{2\nu} + p_{2\mu} p_{1\nu}) C_{12}, \quad (\text{A9})$$

where $\{0, \mu, \mu\nu\}$ stands for an index being 0, μ , or $\mu\nu$ which corresponds to the momentum $\{1, k_\mu, k_\mu k_\nu\}$ being 1, k_μ , or $k_\mu k_\nu$. ϵ is the infinitesimal in Feynman prescription of pole. μ is the 't Hooft parameter as a mass parameter introduced through dimensional regularization. $\epsilon \equiv (4 - d)/2$ is the dimension regulated under the dimensional regularization.

$F_2^{(1)}(0)$ can be extracted from the piece proportional to $(p_1^\mu + p_2^\mu)$ in Eq. (A4), which yields

$$F_2^{(1)}(0) = 4\pi^2 \lambda_l^2 m_l^2 [2C_1(m_l^2, 0, m_l^2, m_\phi^2, m_l^2, m_l^2)$$

$$+ C_{11}(m_l^2, 0, m_l^2, m_\phi^2, m_l^2, m_l^2) + C_{12}(m_l^2, 0, m_l^2, m_\phi^2, m_l^2, m_l^2)].$$

Coefficient functions (C_1 , C_{11} and C_{12}) can be evaluated with *Mathematica* packages, such as PackageX [44, 45]. Then, we get

$$F_2^{(1)}(0) = -\frac{1}{16\pi^2 m_l^4} \lambda_l^2 \left[m_\phi^4 \log\left(\frac{m_\phi^2}{m_l^2}\right) 2m_\phi^2 \sqrt{m_\phi^4 - 4m_\phi^2 m_l^2} \log\left(\frac{m_\phi^2 + \sqrt{m_\phi^4 - 4m_\phi^2 m_l^2}}{2m_\phi m_l}\right) + m_l^2 \left(-3m_\phi^2 \log\left(\frac{m_\phi^2}{m_l^2}\right) - 2m_\phi^2 + 2\sqrt{m_\phi^4 - 4m_\phi^2 m_l^2} \log\left(\frac{m_\phi^2 + \sqrt{m_\phi^4 - 4m_\phi^2 m_l^2}}{2m_\phi m_l}\right) \right) + 3m_l^4 \right], \quad (\text{A10})$$

which is consistent with the result in Ref. [27]. Finally, we find the contribution to δa_l , which is

$$\delta a_{l1}(m_\phi) = \text{Re}(F_2^{(1)}(0)) \equiv \lambda_l^2 a_{sl}(r_l), \quad (\text{A11})$$

with

$$a_{sl}(r_l) = \begin{cases} \frac{-2r_l^2 - 3r_l^2 \log(r_l^2) + r_l^4 \log(r_l^2) - 2\sqrt{4r_l^2 - r_l^4} r_l^2 \cos^{-1}(\frac{r_l}{2}) + 2\sqrt{4r_l^2 - r_l^4} \cos^{-1}(\frac{r_l}{2}) + 3}{16\pi^2} & \text{if } r_l \leq 2, \\ \frac{-2r_l^2 - 3r_l^2 \log(r_l^2) + r_l^4 \log(r_l^2) - 2\sqrt{r_l^4 - 4r_l^2} r_l^2 \cosh^{-1}(\frac{r_l}{2}) + 2\sqrt{r_l^4 - 4r_l^2} \cosh^{-1}(\frac{r_l}{2}) + 3}{16\pi^2} & \text{if } r_l \geq 2, \end{cases} \quad (\text{A12})$$

where $r_l \equiv m_\phi/m_l$ with $l = e, \mu$.

Next, let us calculate the contribution from the

Sacalar-Lepton-Photon loop diagram (Fig. 12). Similar to the first diagram, its amplitude is calculated to be

$$\begin{aligned} \text{Amp02} &= i\pi^2 e \lambda_l \lambda_\gamma (p_1^\mu + p_2^\mu) [B_0(m_l^2, 0, m_l^2) + m_\phi^2 C_0(0, m_l^2, m_l^2, m_\phi^2, 0, m_l^2) - 2m_l^2 C_0(0, m_l^2, m_l^2, m_\phi^2, 0, m_l^2) \\ &- 2m_l^2 C_1(m_l^2, 0, m_l^2, m_l^2, m_\phi^2, 0) - 2m_l^2 C_2(m_l^2, 0, m_l^2, m_l^2, 0, m_\phi^2) \\ &- 2m_l^2 C_{12}(m_l^2, 0, m_l^2, m_l^2, 0, m_\phi^2) - 2m_l^2 C_{12}(m_l^2, 0, m_l^2, m_l^2, m_\phi^2, 0)] (\varphi(p_2, m_l)) \cdot (\varphi(p_1, m_l)) \\ &+ i\pi^2 e \lambda_l \lambda_\gamma [m_\phi^2 p_1^\mu C_1(m_l^2, 0, m_l^2, m_l^2, m_\phi^2, 0) + m_\phi^2 p_2^\mu C_2(m_l^2, 0, m_l^2, m_l^2, 0, m_\phi^2) - 4m_l^2 p_1^\mu C_1(m_l^2, 0, m_l^2, m_l^2, 0, m_\phi^2) \\ &- 4m_l^2 p_2^\mu C_2(m_l^2, 0, m_l^2, m_l^2, m_\phi^2, 0) - 2m_l^2 p_1^\mu C_{11}(m_l^2, 0, m_l^2, m_l^2, 0, m_\phi^2) - 2m_l^2 p_1^\mu C_{11}(m_l^2, 0, m_l^2, m_l^2, m_\phi^2, 0)] \end{aligned} \quad (\text{A13})$$

$$\begin{aligned}
& -2m_l^2 p_2^\mu C_{22}(m_l^2, 0, m_l^2, m_l^2, 0, m_\phi^2) - 2m_l^2 p_2^\mu C_{22}(m_l^2, 0, m_l^2, m_l^2, m_\phi^2, 0)] (\varphi(p_2, m_l)) \cdot (\varphi(p_1, m_l)) \\
& - \frac{i\pi^2 e \lambda_l \lambda_\gamma}{2m_l} [4m_l^2 B_0(m_l^2, m_\phi^2, m_l^2) - 2m_l^2 m_\phi^2 C_0(0, m_l^2, m_l^2, m_\phi^2, 0, m_l^2) - m_l^2 m_\phi^2 C_2(m_l^2, 0, m_l^2, m_l^2, m_\phi^2, 0) - 2A_0(m_l^2) \\
& - m_l^2 m_\phi^2 C_1(m_l^2, 0, m_l^2, m_l^2, 0, m_\phi^2) + m_l^2 m_\phi^2 C_1(m_l^2, 0, m_l^2, m_l^2, m_\phi^2, 0) + m_l^2 m_\phi^2 C_2(m_l^2, 0, m_l^2, m_l^2, 0, m_\phi^2) + A_0(m_\phi^2) \\
& - m_\phi^2 B_0(m_l^2, m_\phi^2, m_l^2) + 4m_l^2 C_{00}(m_l^2, 0, m_l^2, m_l^2, 0, m_\phi^2) + 4m_l^2 C_{00}(m_l^2, 0, m_l^2, m_l^2, m_\phi^2, 0)] (\varphi(p_2, m_l)) \cdot \gamma^\mu \cdot (\varphi(p_1, m_l))
\end{aligned}$$

$F_2^{(2)}(0)$ can be extracted from the piece proportional to $(p_1^\mu + p_2^\mu)$ in Eq. (A13), which turns out to be

$$\begin{aligned}
\frac{ie}{2m_l} (p_1^\mu + p_2^\mu) F_2^{(2)}(0) &= i\pi^2 e \lambda_l \lambda_\gamma (p_1^\mu + p_2^\mu) [B_0(m_l^2, 0, m_l^2) + m_\phi^2 C_0(0, m_l^2, m_l^2, m_\phi^2, 0, m_l^2) \\
& - 2m_l^2 C_0(0, m_l^2, m_l^2, m_\phi^2, 0, m_l^2) - 2m_l^2 C_1(m_l^2, 0, m_l^2, m_l^2, m_\phi^2, 0) - 2m_l^2 C_2(m_l^2, 0, m_l^2, m_l^2, 0, m_\phi^2) \\
& - 2m_l^2 C_{12}(m_l^2, 0, m_l^2, m_l^2, 0, m_\phi^2) - 2m_l^2 C_{12}(m_l^2, 0, m_l^2, m_l^2, m_\phi^2, 0)] (\varphi(p_2, m_l)) \cdot (\varphi(p_1, m_l)) \\
& + i\pi^2 e \lambda_l \lambda_\gamma [m_\phi^2 p_1^\mu C_1(m_l^2, 0, m_l^2, m_l^2, m_\phi^2, 0) + m_\phi^2 p_2^\mu C_2(m_l^2, 0, m_l^2, m_l^2, 0, m_\phi^2) - 4m_l^2 p_1^\mu C_1(m_l^2, 0, m_l^2, m_l^2, 0, m_\phi^2) \\
& - 4m_l^2 p_2^\mu C_2(m_l^2, 0, m_l^2, m_l^2, m_\phi^2, 0) - 2m_l^2 p_1^\mu C_{11}(m_l^2, 0, m_l^2, m_l^2, 0, m_\phi^2) - 2m_l^2 p_1^\mu C_{11}(m_l^2, 0, m_l^2, m_l^2, m_\phi^2, 0) \\
& - 2m_l^2 p_2^\mu C_{22}(m_l^2, 0, m_l^2, m_l^2, 0, m_\phi^2) - 2m_l^2 p_2^\mu C_{22}(m_l^2, 0, m_l^2, m_l^2, m_\phi^2, 0)]
\end{aligned} \tag{A14}$$

After coefficient functions are evaluated with PackageX [44, 45], we get

$$\begin{aligned}
F_2^{(2)}(0) &= -\frac{1}{48\pi^2 m_l^3} \lambda_l \lambda_\gamma \left[m_\phi^4 \log\left(\frac{m_\phi^2}{m_l^2}\right) - 2m_\phi^2 \sqrt{m_\phi^4 - 4m_\phi^2 m_l^2} \log\left(\frac{m_\phi^2 + \sqrt{m_\phi^4 - 4m_\phi^2 m_l^2}}{2m_\phi m_l}\right) \right. \\
& \left. - m_l^2 \left(6m_\phi^2 \log\left(\frac{m_\phi^2}{m_l^2}\right) + 2m_\phi^2 - 8\sqrt{m_\phi^4 - 4m_\phi^2 m_l^2} \log\left(\frac{m_\phi^2 + \sqrt{m_\phi^4 - 4m_\phi^2 m_l^2}}{2m_\phi m_l}\right) \right) + 6m_l^4 \left(\log\left(\frac{\mu^2}{m_l^2}\right) + 3 + \frac{1}{\epsilon} \right) \right],
\end{aligned} \tag{A15}$$

where $\frac{1}{\epsilon} \equiv \frac{1}{\epsilon} - \gamma + \log(4\pi)$ with the Euler's constant γ . The term, $-\frac{\lambda_l \lambda_\gamma m_l}{8\pi^2} \frac{1}{\epsilon}$, is the regularized UV divergence which can be cancelled at low energy. The IR part, $-\frac{\lambda_l \lambda_\gamma m_l}{8\pi^2} \log\left(\frac{\mu^2}{m_l^2}\right)$, can be cancelled by the bremsstrahlung effect. Finally, we arrive at

$$\delta a_{l2}(m_\phi) = \text{Re}(F_2^{(2)}(0)) \equiv \lambda_l \lambda_\gamma m_l b_{sl\gamma}(r_l), \tag{A16}$$

where

$$b_{sl\gamma}(r_l) = \begin{cases} \frac{-2r_l^2 - 6r_l^2 \log(r_l^2) + r_l^4 \log(r_l^2) - 2\sqrt{4r_l^2 - r_l^4} r_l^2 \cos^{-1}\left(\frac{r_l}{2}\right) + 8\sqrt{4r_l^2 - r_l^4} \cos^{-1}\left(\frac{r_l}{2}\right) + 18}{48\pi^2} & \text{if } r_l \leq 2, \\ \frac{-2r_l^2 - 6r_l^2 \log(r_l^2) + r_l^4 \log(r_l^2) - 2\sqrt{r_l^4 - 4r_l^2} r_l^2 \cosh^{-1}\left(\frac{r_l}{2}\right) + 8\sqrt{r_l^4 - 4r_l^2} \cosh^{-1}\left(\frac{r_l}{2}\right) + 18}{48\pi^2} & \text{if } r_l \geq 2. \end{cases} \tag{A17}$$

Appendix B: Calculation of contribution of the scalar ϕ to η

For the scalar model (4), the ϕ contribution to the Eötvs parameter has been calculated in Refs. [13, 37].

Here, we quote their results as following. It is straightforward to check that the Newtonian interaction between

a mass A and a mass B will be modified into the form

$$V = -\frac{Gm_A m_B}{r_{AB}}(1 + \zeta_A \zeta_B e^{-r_{AB}/\Lambda_\phi}), \quad (\text{B1})$$

where G is the Newtonian constant. $\Lambda_\phi \equiv \hbar/m_\phi$ is the Compton wavelength of the scalar ϕ .

ζ_A is the so-called scalar-charge for a mass. The scalar model leads to the ϕ -dependence for lepton and quark masses. Ordinary matter is made of atoms, which can be further decomposed into fundamental particles (photons, electrons, gluons and quarks). Thus, the scalar model (4) leads to the ϕ -dependence for atomic mass, which gives the definition for ζ_A ,

$$\zeta_A = -\kappa^{-1} \left[\lambda_g + \frac{1}{m_A} \left((\lambda_{\hat{m}} - \lambda_g \hat{m}) \frac{\partial m_A}{\partial \hat{m}} - 4\lambda_\gamma \alpha \frac{\partial m_A}{\partial \alpha} \right) + (\lambda_{\delta m} - \lambda_g \delta m) \frac{\partial m_A}{\partial \delta m} + (\lambda_{m_e} - \lambda_g m_e) \frac{\partial m_A}{\partial m_e} \right], \quad (\text{B2})$$

where $\hat{m} = \frac{m_d + m_u}{2}$, $\delta m = m_d - m_u$, $\lambda_{\hat{m}} = \frac{\lambda_d + \lambda_u}{2}$, and $\lambda_{\delta m} = \lambda_d - \lambda_u$.

The calculation of ζ_A is quite complicated, which has been done in Ref. [13],

$$\begin{aligned} \zeta_A &= -\kappa^{-1} \left[\lambda_g + \left(\frac{\lambda_{\hat{m}}}{\hat{m}} - \lambda_g \right) Q_{\hat{m}} + \left(\frac{\lambda_{\delta m}}{\delta m} - \lambda_g \right) Q_{\delta m} \right. \\ &\quad \left. + \left(\frac{\lambda_e}{m_e} - \lambda_g \right) Q_{m_e} - 4\lambda_\gamma Q_e \right] \\ &= -\kappa^{-1} \left[(1 - Q_{\hat{m}} - Q_{\delta m} - Q_{m_e}) \lambda_g + \frac{\lambda_e}{m_e} Q_{m_e} - 4\lambda_\gamma Q_e \right. \\ &\quad \left. + \left(\frac{Q_{\hat{m}}}{m_d + m_u} + \frac{Q_{\delta m}}{m_d - m_u} \right) \lambda_d + \left(\frac{Q_{\hat{m}}}{m_d + m_u} - \frac{Q_{\delta m}}{m_d - m_u} \right) \lambda_u \right] \end{aligned}$$

where

$$Q_{\hat{m}} = F_A \left[0.093 - \frac{0.036}{A^{1/3}} - 0.02 \frac{(A - 2Z)^2}{A^2} \right.$$

$$\left. - 1.4 \times 10^{-4} \frac{Z(Z-1)}{A^{4/3}} \right] \quad (\text{B4a})$$

$$Q_{\delta m} = F_A \left[0.0017 \frac{A - 2Z}{A} \right] \quad (\text{B4b})$$

$$Q_{m_e} = F_A \left[5.5 \times 10^{-4} \frac{Z}{A} \right], \quad (\text{B4c})$$

and

$$Q_e = F_A \left[-1.4 + 8.2 \frac{Z}{A} + 7.7 \frac{Z(Z-1)}{A^{4/3}} \right] \times 10^{-4}. \quad (\text{B4d})$$

Z is the atomic number, and A is the mass number of atoms. The factor F_A can be replaced by one in lowest approximation.

For two test bodies freely falling towards the Earth, the Eötvös parameter η is found to be [37]

$$\eta = \frac{\left(1 + \frac{R_E}{\Lambda_\phi} \right) I \left(\frac{R_E}{\Lambda_\phi} \right) (\zeta_A - \zeta_B) \zeta_E e^{-R_E/\Lambda_\phi}}{I(x) \equiv \frac{3(x \cosh(x) - \sinh(x))}{x^3}}, \quad (\text{B5})$$

where R_E is the radius of the Earth. Here, the factor $I(x)$ takes into account the fact that the Earth is a sphere of finite size. According to Ref. [46], the Earth is made of 49.83% Oxygen, 15.19% Iron, 15.14% Magnesium, 14.23% Silicon, 2.14% Sulfur, 1.38% Aluminum and 1% Calcium. Then, one can calculate the scalar-charge of the Earth,

$$\begin{aligned} \zeta_E &= -1.808 \times 10^{18} \lambda_e + 2.319 \times 10^{25} \lambda_\gamma \cdot \text{eV} \quad (\text{B6}) \\ &\quad - 3.133 \times 10^{27} \lambda_g \cdot \text{eV} - 3.973 \times 10^{19} \lambda_d - 3.967 \times 10^{19} \lambda_u. \end{aligned}$$

-
- [1] R. D. Peccei and H. R. Quinn, *Phys. Rev. Lett.* **38**, 1440 (1977).
[2] S. Weinberg, *Phys. Rev. Lett.* **40**, 223 (1978).
[3] F. Wilczek, *Phys. Rev. Lett.* **40**, 279 (1978).
[4] R. Essig *et al.*, arXiv: 1311.0029, and references therein.
[5] B. Patt and F. Wilczek, (2006), arXiv:hep-ph/0605188.
[6] D. O'Connell, M. J. Ramsey-Musolf, and M. B. Wise, *Phys. Rev. D* **75**, 037701 (2007).
[7] V. Barger, P. Langacker, M. McCaskey, M. J. Ramsey-Musolf, and G. Shaughnessy, *Phys. Rev. D* **77**, 035005 (2008).
[8] F. Piazza and M. Pospelov, *Phys. Rev. D* **82**, 043533 (2010).
[9] J. P. Conlon, *J. High Energy Phys.* **2006** (05), 078.
[10] P. Svrcek and E. Witten, *J. High Energy Phys.* **2006** (06), 051.
[11] A. Arvanitaki, S. Dimopoulos, S. Dubovsky, N. Kaloper, and J. March-Russell, *Phys. Rev. D* **81**, 123530 (2010).
[12] C. Brans and R. H. Dicke, *Phys. Rev.* **124**, 925 (1961).
[13] T. Damour and J. F. Donoghue, *Phys. Rev. D* **82**, 084033 (2010).
[14] M. Battaglieri *et al.*, arXiv: 1707.04591.
[15] S. Navas *et al.* (Particle Data Group Collaboration), *Phys. Rev. D* **110**, 030001 (2024), Section 90.
[16] T. Aoyama, M. Hayakawa, T. Kinoshita, and M. Nio, *Phys. Rev. Lett.* **109**, 111807 (2012).
[17] T. Aoyama, T. Kinoshita, and M. Nio, *Atoms* **7**, 28 (2019).
[18] S. Volkov, arXiv: 2404.00649.
[19] T. Aoyama, M. Hayakawa, T. Kinoshita, and M. Nio, *Phys. Rev. Lett.* **109**, 111808 (2012).
[20] T. Aoyama *et al.*, *Phys. Rept.* **887**, 1 (2020).
[21] G. Colangelo *et al.*, arXiv: 2203.15810.
[22] R. H. Parker, C. Yu, W. Zhong, B. Estey, and H. Müller,

- Science **360**, 191 (2018).
- [23] L. Morel, Z. Yao, P. Cladé, and S. Guellati-Khélifa, *Nature* **588**, 61 (2020).
- [24] X. Fan, T. G. Myers, B. A. D. Sukra, and G. Gabrielse, *Phys. Rev. Lett.* **130**, 071801 (2023).
- [25] D. P. Aguillard *et al.* (The Muon $g - 2$ Collaboration), *Phys. Rev. Lett.* **131**, 161802 (2023).
- [26] D. Chang, W.-F. Chang, C.-H. Chou, and W.-Y. Keung, *Phys. Rev. D* **63**, 091301 (2001).
- [27] C.-Y. Chen, H. Davoudiasl, W. J. Marciano, and C. Zhang, *Phys. Rev. D* **93**, 035006 (2016).
- [28] W. J. Marciano, A. Masiero, P. Paradisi, and M. Passera, *Phys. Rev. D* **94**, 115033 (2016).
- [29] J. Bergé, P. Brax, G. Métris, M. Pernot-Borràs, P. Touboul, and J.-P. Uzan, *Phys. Rev. Lett.* **120**, 141101 (2018).
- [30] P. Touboul *et al.* (MICROSCOPE Collaboration), *Phys. Rev. Lett.* **129**, 121102 (2022).
- [31] P. Touboul *et al.* (MICROSCOPE Collaboration), *Class. Quant. Grav.* **39**, 204009 (2022).
- [32] J. Bergé, *Rept. Prog. Phys.* **86**, 066901 (2023).
- [33] K. Beloy *et al.* (Boulder Atomic Clock Optical Network (BACON)), *Nature* **591**, 564 (2021).
- [34] S. M. Vermeulen *et al.*, *Nature* **600**, 424 (2021).
- [35] G. Passarino and M. Veltman, *Nucl. Phys. B* **160**, 151 (1979).
- [36] G. 't Hooft and M. Veltman, *Nucl. Phys. B* **153**, 365 (1979).
- [37] W. Zhao, D. Gao, J. Wang, and M. Zhan, *Gen. Relat. Grav.* **54**, 41 (2022).
- [38] G. F. Giudice, P. Paradisi, and M. Passera, *J. High Energy Phys.* **2012** (11), 113.
- [39] C. Struckmann, R. Corgier, S. Loriani, G. Kleinsteinberg, N. Gox, E. Giese, G. Métris, N. Gaaloul, and P. Wolf, *Phys. Rev. D* **109**, 064010 (2024).
- [40] M. Nowakowski, E. A. Paschos, and J. M. Rodríguez, *Eur. J. Phys.* **26**, 545 (2005).
- [41] R. Mertig, M. Böhm, and A. Denner, *Comp. Phys. Comm.* **64**, 345 (1991).
- [42] V. Shtabovenko, R. Mertig, and F. Orellana, *Comp. Phys. Comm.* **256**, 107478 (2020).
- [43] T. Hahn, *Comp. Phys. Comm.* **140**, 418 (2001).
- [44] H. H. Patel, *Comp. Phys. Comm.* **197**, 276 (2015).
- [45] H. H. Patel, *Comp. Phys. Comm.* **218**, 66 (2017).
- [46] J. W. Morgan and E. Anders, *Proc. Natl. Acad. Sci. USA* **77**, 6973 (1980).